Ruthenium and platinum catalyzed carbon oxidation: A comparative kinetic study

M. Jeguirim [a,*], K. Villani [b], J.F. Brilhac [a], J.A. Martens [b]

[a] Laboratoire Gestion des Risques et Environnement, Université de Haute Alsace 25, rue de Chemnitz, 68200 Mulhouse, France
[b] Department of Microbial and Molecular Systems, Centrum voor Oppervlaktechemie en Katalyse (C.O.K.), K.U. Leuven, Kasteelpark Arenberg 23, B-3001 Leuven, Belgium

ABSTRACT

Carbon oxidation catalyzed by Ru/Na-Y zeolite under conditions relevant to automotive exhaust gas after treatment was experimentally investigated. In the presence of Ru/Na-Y zeolite catalyst carbon oxidation can be described by three mechanisms, viz. (i) reaction between carbon and NO_2; (ii) reaction between carbon and O_2 and (iii) cooperative reaction of carbon involving O_2 and NO_2 simultaneously. The kinetic analysis suggested that the direct $C–O_2$ and the cooperative $C–NO_2–O_2$ reaction in the presence of Ru/Na-Y catalyst proceeded according to the adsorption of oxygen on carbon surface followed by a decomposition of these oxygenate surface complexes. The kinetic description of the Ru/Na-Y zeolite catalyst is compared with kinetic models of platinum based carbon oxidation from literature. The catalytic properties of ruthenium and platinum based catalysts were found to be fundamentally different. On the ruthenium catalyst the activation energy for the cooperative $C–O_2–NO_2$ reaction and the direct $C–O_2$ reaction is similar, whereas on platinum, the direct $C–O_2$ reaction is slower. In the presence of platinum catalyst NO_2 molecules intervene in the decomposition of surface oxygenated carbon complexes, formed by the oxygen adsorption on carbon surface. The kinetic models based on the occurring of direct and cooperative reactions may be applied for the catalytic oxidation of soot in the regenerative particle trap conditions.

© 2010 Elsevier B.V. All rights reserved.

1. Introduction

For compliance with present and future emission limits of diesel particulate matter (DPM), a variety of particle trapping and exhaust treatment technologies have been introduced [1–3]. However, these technologies generally require the regeneration of the filter by oxidative removal of carbonaceous particles. Essentially two approaches to trapped soot combustion have been considered, viz. passive and active regeneration [4].

The active regeneration technology is based on discontinuous oxidation by O_2 at temperatures higher than ca. 420 °C by a secondary energy supply to heat the exhaust gas. The addition of a ceria-based fuel-born catalyst leads to a lowering of the particulate matter combustion temperature by approximately 100 °C [5,6]. Active systems involve a fuel penalty or bear the danger of additional potentially hazardous emission. Passive systems seem to be a convenient way to increase the time interval between regenerations provided high catalytic activity can be maintained. Passive technology is based on a continuous oxidation at temperatures in the range of 250–400 °C with NO_2 as the main oxidant. The regeneration of monolithic wall-flow filters by NO_2 generated in an upstream oxidation catalyst was developed by

Cooper and Thoss [7]. It has been commercialized as the "continuously regenerating trap (CRT)" system [8]. Several investigations on the chemistry of the soot oxidation reaction in the combination $C–NO_2–O_2$ system have been published [9–15]. The $C–NO_2–O_2$ reaction global mechanism in the absence of catalyst is well established [12–14] and consists in two main reactions taking place simultaneously: a direct reaction between carbon and NO_2 (Eqs. (1a) and (1b)) and a cooperative one involving simultaneously O_2 and NO_2 (Eqs. (2a) and (2b)). The global mechanism may be written as follows:

$$C + 2NO_2 \rightarrow CO_2 + 2NO \tag{1a}$$

$$C + NO_2 \rightarrow CO + NO \tag{1b}$$

$$C + NO_2 + \tfrac{1}{2}O_2 \rightarrow CO_2 + NO \tag{2a}$$

$$C + NO_2 + \tfrac{1}{2}O_2 \rightarrow CO + NO_2 \tag{2b}$$

For the cooperative reactions (Eqs. (2a) and (2b)), NO_2 adsorbs on the surface oxygenated carbon complexes (SOCs), which are formed through O_2 chemisorption and reacts to give rise to formation of carboxyl, lactone, and anhydride functional groups as observed by Setiabudi et al. [21]. These functional groups react further with NO_2 leading to the emission of CO and CO_2. For the direct reactions (Eqs. (2a) and (2b)), it was shown that the

* Corresponding author. Tel.: +33 3 89327658; fax: +33 3 89327661.
E-mail address: mejdi.jeguirim@uha.fr (M. Jeguirim).

Table 1
Elemental analysis (wt%) of carbon black Vulcan 6.

	Elemental analysis (wt%)						Surface area (m²/g)	Apparent density (kg/m³)	Mean particle diameter (nm)
	C	H	N	O	S	Ash			
CB	95.2	0.7	<0.3	2.1	1.0	0	106	364	20

oxidation rate is increased in the presence of water vapor [13–15]. The establish mechanism shows the formation of a small amounts of nitric and nitrous acid leading to the increase of nitro-oxygenated species on carbon surface [15].

Alternatively, soot combustion may be increased with the help of catalytic oxidation. This may be accomplished by impregnating the filter surface with catalyst, which minimizes operational risks and energy consumption [2,4]. Different catalysts have been tested for diesel soot combustion [16–23]. Among these catalysts, it was reported that platinum is quite efficient for the catalytic oxidation of soot under passive regeneration conditions [19–23]. The global mechanism of the catalytic oxidation of soot by NO_2 and O_2 in the presence of Pt catalyst was well established [24]. It was shown that, besides the well known catalytic re-oxidation of NO into NO_2, Pt also exerts a catalytic effect on the cooperative carbon–NO_2–O_2 oxidation reaction. Pt catalyst acts on the cooperative reaction by enhancing the formation of atomic oxygen species which are transferred to the carbon surface. A kinetic model of the catalytic oxidation of soot was built based on the established global mechanism. The kinetic equations indicated that the frequency factor of the cooperative reaction is increased in the presence of Pt. These results confirm that the Pt catalyst contributes to the formation of SOCs [24,25].

More recently, a few studies have been devoted to the oxidation of soot in the presence of Ru based catalyst [26–29]. A comparison between ruthenium and platinum based catalysts in C–O_2 [26] and C–NO_2 [27] reactions showed that Ru catalysts are more active in both types of reactions compared to Pt based catalyst. Those investigations evidenced the potential of ruthenium to decompose NO_2 and O_2 into reactive oxygen species that are spilled-over to the carbon surface. SOCs were shown to be decomposed in the presence of NO_2 leading to an increase of the carbon oxidation rate [26–29].

The purpose of this work was to determine kinetic expressions for describing the catalytic oxidation of carbon by NO_2 and O_2 in the presence of Ru/Na-Y catalyst, using the same mono-dimensional model previously established for the catalytic oxidation of carbon by NO_2 and O_2 in the presence of Pt catalyst. The kinetic constants of Ru and Pt catalysts are compared and fundamental differences of both types of noble metals revealed.

2. Experimental

The Ru/Na-Y catalyst used in this study was prepared by cationic exchange. Na-Y zeolite (Si/Al ratio 2.71) obtained from Zeocat was loaded with 3 wt% ruthenium by slurring zeolite powder in an aqueous solution of $RuCl_3$ (Alfa Aesar) at 80 °C. The pH was maintained at 8.5 by addition of ammonia to avoid precipitation. The quantitative uptake of ruthenium was confirmed using ICP of the filtrate and analysis of dissolved ruthenium zeolite using the same technique. The catalyst powder was filtered, washed with de-ionized water and dried at 60 °C. Pretreatment of the Ru-exchanged Na-Y zeolite was done at 500 °C in flowing nitrogen. TEM investigations revealed that the Ru metal is finely dispersed, especially over the external surface of the zeolite particles [23].

A commercial carbon black Vulcan 6 suitable as a model soot (106 m²/g) was used in this study. Experiments with model soot

have been reported in several laboratory studies. Gray and Do have used a commercial activated carbon (Norit RB) as a standard for the study of the dynamics of the nitrogen dioxide reaction with the carbon and to monitor the formation of carbon surface oxygen complexes [30]. Setiabudi et al. have investigated the reaction NO_2 and Printex U (Degussa) in the presence of catalysts to study the soot oxidation rates with NO_2 in diesel particulate catalytic filter [21]. The use of commercial soot for laboratory studies is being favoured since it can be obtained in large quantities with reproducible characteristics. The elemental analysis of the commercial CB Vulcan 6 used in this present investigation is shown in Table 1.

Isothermal experiments of carbon oxidation in the presence of Ru/Na-Y were carried out in a fixed bed described in Fig. 1. For each catalytic test, 50 mg of carbon black (Vulcan 6) were physically mixed with 50 mg Ru/Na-Y catalyst, and crushed in a mortar for 20 min. The obtained sample was placed on a quartz frit ($d = 16$ mm) set in a vertical fused silica tube. The fixed bed was heated by an electrical furnace driven by a temperature programmer controller. Gas temperature was measured by a thermocouple located 1 mm above the studied sample. In a typical run the sample was heated under pure He to the reaction temperature and then the gas flow was switched to the reactive gas mixture containing 0–400 ppmv NO_2, 0–10%b.v. O_2 in He. In all experiments a total flow rate equal to 100 NL/h was used at 1 atm. Experiments were performed under isothermal conditions in the temperature range 300–400 °C. The mole fractions of NO_2, NO, CO_2 and CO were measured continuously at the reactor outflow. Carbon oxide concentrations were measured using a Maihak Multor 610 gas analyser (infra-red absorption); nitrogen oxide concentrations using a Rosemount NGA 2000 gas analyser (chemiluminescence). Before each measurement period, the gas analysers were calibrated with reference gases (Air Liquid Special Gas, tolerance ±2%).

The specific oxidation rate of carbon r, expressed in mg/s/g$_{Ci}$, was calculated for a carbon mass conversion of 20% from the total
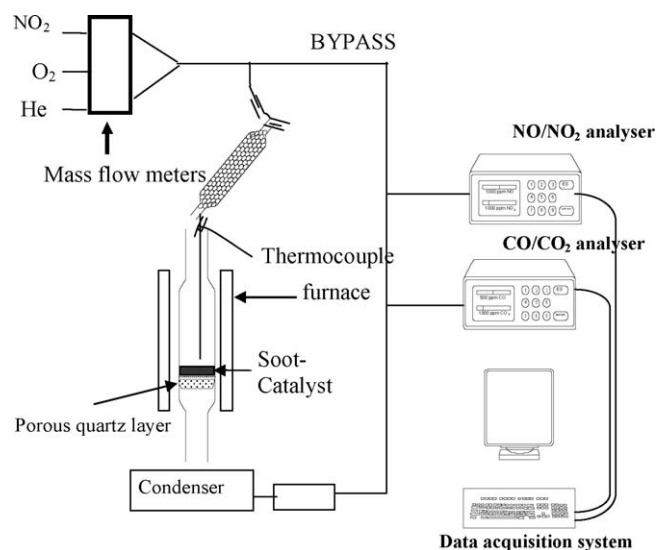

Fig. 1. Scheme of the set-up for the fixed bed experiments.

gas flow rate and the amounts of CO and CO_2 released during reaction at the outlet of the reactor using the following equation:

$$-\frac{1}{m_i}\frac{dm}{dt} = (X_{CO} + X_{CO_2}) \times F \times M_C \times 10^3 \qquad (3)$$

in which X_{CO} and X_{CO_2} are the measured molar fraction of these species in the gas phase, F is the molar flow of gases through the reactor, m_i and M_C are the initial and the molar mass of carbon, respectively. Previous studies have shown that under these experimental conditions the reaction proceeds in the kinetic regime [9,13,24]. Moreover, Messerer et al. observed that the rate constant k of the soot oxidation by NO_2 and O_2 was constant for carbon mass conversions of 20–75% under similar experimental conditions as applied here [9].

3. Kinetic model of carbon oxidation by NO_2 and O_2 in the presence of Ru/Na-Y catalyst

Previous investigations have shown that the global mechanism for the carbon oxidation by NO_2 and O_2 in the presence of Ru/Na-Y catalyst may be written as follows [27,29]:

$$C + O_2 \rightarrow CO_2 \qquad (4)$$

$$C + NO_2 \rightarrow CO + NO \qquad (5)$$

$$C + 2NO_2 \rightarrow CO_2 + 2NO \qquad (6)$$

$$C + \tfrac{1}{2}O_2 + NO_2 \rightarrow CO + NO_2 \qquad (7)$$

$$C + O_2 + NO_2 \rightarrow CO_2 + NO_2 \qquad (8)$$

Reactions (4), (6) and (8) are catalyzed by Ru.

The C–NO_2–O_2 reaction in the absence and in the presence of Pt catalyst is well documented [24,25]. Similarly, the overall gasification reaction of carbon upon reacting with NO_2–O_2 mixture in the presence of Ru/Na-Y catalyst can be presented as being the combined effect of the direct C–O_2 reaction, the C–NO_2 reaction and the cooperative C–NO_2–O_2 reaction. The overall carbon gasification rate, r is expressed as follows:

$$r = r_{dirO_2} + r_{dirNO_2} + r_{coop} \qquad (9)$$

where r_{dirO_2}, r_{dirO_2} and r_{coop} are the intrinsic carbon gasification rate for the direct C–O_2, C–NO_2 reactions and cooperative C–NO_2–O_2 reaction respectively.

The kinetic equation corresponding to the direct C–O_2 reaction in the presence of Ru/Na-Y catalyst may be expressed as follows:

$$r_{dirO_2} = k_{dirO_2}^{cat} X_{O_2}^{\alpha} \qquad (10)$$

in which $k_{dirO_2}^{cat}$ is the intrinsic rate constant for reaction (4), X_{O_2} is the local volumetric fraction of O_2 and α is the reaction order with respect to O_2. This expression includes one term corresponding to the evolution of CO_2. Formation of CO was not considered since experimentally the oxidation of carbon by oxygen in the presence of Ru/Na-Y catalyst did not lead to CO formation [29].

However, both r_{dirNO_2} and r_{coop} include two terms corresponding to the evolution of CO and CO_2 since both gases were emitted during the C–NO_2 and C–NO_2–O_2 reaction [27,29]. As shown in our previous studies [13,24,25], the kinetical equations corresponding to the direct oxidation reaction (Eqs. (5) and (6)) of the catalyzed system may be written as follows:

$$r_{dir} = k_{CO_2}^{cat} X_{NO_2}^{\beta} + k_{CO} X_{NO_2}^{\beta'} \qquad (11)$$

in which k_{CO} and $k_{CO_2}^{cat}$ are the rate constants for Eqs. (5) and (6), X_{NO_2} is the local volumetric fraction of NO_2, β' and β are the reaction orders with respect to NO_2 for Eq. (5) and (6), respectively.

In a similar way, the kinetic equations corresponding to the cooperative oxidation reaction (Eqs. (7) and (8)) of the catalyzed system may be written as follows:

$$r_{coop} = k_{O_2,CO_2}^{cat} X_{NO_2}^{\delta} X_{O_2}^{\chi} + k_{O_2,CO} X_{NO_2}^{\delta'} X_{O_2}^{\chi'} \qquad (12)$$

in which $k_{O_2,CO}$ and k_{O_2,CO_2}^{cat} are the intrinsic rate constants for reactions (7) and (8) respectively. X_{NO_2} is the local volumetric fraction of NO_2, X_{O_2} is the local volumetric fraction of O_2 and δ, δ' and χ, χ' are the reaction orders with respect to NO_2 and O_2. The dependence of the different rate constants on temperature is expressed by an Arrhenius function:

$$k = A \exp\left(\frac{-E_a}{RT}\right) \qquad (13)$$

in which A and E_a are the pre-exponential factor and the apparent activation energy respectively. R is the molar gas constant.

The intrinsic rate constants $k_{dirO_2}^{cat}$, k_{CO}, $k_{CO_2}^{cat}$, $k_{O_2,CO}$ and k_{O_2,CO_2}^{cat} were determined using a mono-dimensional model of the reaction through the fixed bed as reported elsewhere [24,25]. The kinetic equations are based on the following assumptions:

- The catalyst-carbon bed is fixed and isothermal;
- A pseudo-steady state regime is considered;
- The pressure P is equal to 1 atm. Pressure, gas flow rate and oxygen mole fraction are considered to be uniform over the entire bed;
- There is no radial concentration gradient and only the bed depth is considered as coordinate of a linear model;
- Only convection is considered in the gas transportation process. NO_2 internal diffusion within the cake is not considered. The Peclet number is close to 100 under our experimental conditions;
- The gradient of NO_2 concentration along the bed thickness is taken into consideration. During its flow through the fixed bed consumption of NO_2 occurs without any re-oxidation of NO into NO_2 through the carbon catalyst layer. In fact, previous investigations on this Ru catalyst showed that, in contrast with the behavior of a Pt catalyst, no significant re-oxidation of the NO into NO_2 is observed during soot oxidation by NO_2 and O_2 [29].

Therefore, the determination of the rate constants was done according to the same procedure as for the uncatalyzed case. Hence, the carbon bed was split into infinitesimal layers.

The mass balance of NO_2, NO, CO and CO_2 species in the inlet and outlet of each layer (δm is the local mass, dz is the layer height, $F_v(T)$ is the flow, $V_m(T)$ is molar volume, M_c is the carbon molar mass) is obtained as follows:

$$\frac{F_v(T)}{V_m(T)} X_{NO_2}|_{z+dz} dt = \frac{F_v(T)}{V_m(T)} X_{NO_2}|_z dt - \frac{\delta m|_z}{M_c} dt \left[2k_{CO_2}^{cat} X_{NO_2}^{\beta} + k_{CO} X_{NO_2}^{\beta'} \right]$$

$$\frac{F_v(T)}{V_m(T)} X_{NO}|_{z+dz} dt = \frac{F_v(T)}{V_m(T)} X_{NO}|_z dt + \frac{\delta m|_z}{M_c} dt \left[2k_{CO_2}^{cat} X_{NO_2}^{\beta} + k_{CO} X_{NO_2}^{\beta'} \right]$$

$$\frac{F_v(T)}{V_m(T)} X_{CO_2}|_{z+dz} dt = \frac{F_v(T)}{V_m(T)} X_{CO_2}|_z dt$$
$$+ \frac{\delta m|_z}{M_c} dt \left[k_{dirO_2}^{cat} X_{O_2}^{\alpha} + 2k_{CO_2}^{cat} X_{NO_2}^{\beta} + k_{O_2,CO_2}^{cat} X_{NO_2}^{\delta} X_{O_2}^{\chi} \right]$$

$$\frac{F_v(T)}{V_m(T)} X_{CO}|_{z+dz} dt = \frac{F_v(T)}{V_m(T)} X_{CO}|_z dt$$
$$+ \frac{\delta m|_z}{M_c} dt \left[k_{CO} X_{NO_2}^{\beta'} + k_{O_2,CO} X_{NO_2}^{\delta'} X_{O_2}^{\chi'} \right]$$

The expression of the specific rate of carbon oxidation in each layer is:

$$-\frac{1}{\partial m}\frac{d(\partial m)}{dt} = k_{dirO_2}^{cat}X_{O_2}^{\alpha} + k_{CO_2}^{cat}X_{NO_2}^{\beta}|_z + k_{CO}X_{NO_2}^{\beta'}|_z + k_{O_2,CO_2}^{cat}X_{NO_2}^{\delta}|_zX_{O_2}^{\chi}$$
$$+ k_{O_2,CO}X_{NO_2}^{\delta'}|_zX_{O_2}^{\chi'}$$

The fraction of consumed carbon concentration is determined in each elementary layer of the fixed bed using input values for the intrinsic rates constants and reaction orders. The outlet CO_2 and CO concentrations were calculated by summing up the carbon consumption in each layer. The retained values of the rate constants, $k_{dirO_2}^{cat}$, $k_{CO_2}^{cat}$, k_{CO}, k_{O_2,CO_2}^{cat}, $k_{O_2,CO}$ and of the reaction orders α, β, β', δ, δ', χ, χ' are those leading to the best agreement with the experimental data of carbon oxidation, as well as of CO, CO_2, NO and NO_2 emissions.

The kinetic constants for the intrinsic oxidation rate in the absence of catalyst and in the presence of Pt catalyst obtained from previous investigations using the same approach are given in Tables 2 and 3, respectively. One may remind that CO was not significantly formed in the presence of Pt catalyst.

4. Results and discussion

4.1. Kinetics of the direct C–O_2 in the presence of Ru/Na-Y catalyst

The oxidation reaction of soot by 10% O_2 in the presence of Ru/Na-Y proceeds at temperatures below 400 °C [29]. In that study [29] significant CO_2 emission during carbon oxidation by 10% O_2 in the presence of Ru/Na-Y was reported. There was almost no formation of CO in the C–O_2 reaction in the presence of Ru/Na-Y catalyst [29].

In order to determine the reaction order with respect to oxygen for the direct C–O_2 reaction in the presence of Ru/Na-Y catalyst, the effect of the inlet oxygen mole fraction on the specific carbon oxidation rate was investigated. Fig. 2 shows that the specific oxidation rate of carbon increased with the inlet oxygen mole fraction at 400 °C. This increase was linear and the reaction order seems to be close to 1.

Experiments of carbon oxidation by O_2 in the presence of Ru/Na-Y allowed to describe the temperature dependence of the kinetic equation as follows:

$$r_{dirO_2} = k_{dirO_2}^{cat}, \qquad X_{O_2}^{\alpha} = 563.23 \exp\left(\frac{-84520}{RT}\right)X_{O_2} \qquad (14)$$

The value of the activation energy obtained for the oxidation of carbon by O_2 in the presence of Ru/Na-Y catalyst (84.5 kJ/mol) was lower than the one reported in literature for the uncatalyzed reaction (170 kJ/mol) [16]. It confirmed the catalytic effect of Ru/Na-Y catalyst on the direct oxidation of carbon in the presence of oxygen.

4.2. Kinetics of direct C–NO_2 in the presence of Ru/Na-Y catalyst

Experiments of carbon oxidation NO_2 revealed a catalytic effect of Ru/Na-Y catalyst at 350 °C and above. The promoting factor of the C–NO_2 reaction by Ru/Na-Y defined as the ratio between the carbon oxidation rate in the presence and in the absence of catalyst is ranging from 1.1 to 1.25 in the temperature range 350–400 °C. This beneficial effect of the catalyst was attributed to the formation of atomic oxygen species through catalytic decomposition of NO_2 on Ru surface sites which are transferred to the carbon surface leading to the formation of SOCs [27].

In order to verify the reaction order with respect to NO_2 for the direct C–NO_2 reaction in the presence of Ru/Na-Y catalyst, the effect of the NO_2 inlet mole fraction on the specific carbon

Table 2
Kinetic constants for the direct and the cooperative reaction in the absence of catalyst.

		k (s^{-1})	E_a (kJ/mol)	A (s^{-1})
Direct reaction	CO_2		45.5	101.3
	CO		59.4	567.3
Cooperative reaction	O_2, CO_2		65.4	1.82×10^4
	O_2, CO		82.6	2.33×10^5

Table 3
Kinetic constants for the direct and the cooperative reaction in the presence of Pt catalyst.

	k (s^{-1})	E_a (kJ/mol)	A
Direct reaction	k_{dir}	49.5	303.9
Cooperative reaction	k_{coop}	72.1	1819.4

oxidation rate was investigated. Fig. 3 shows that the specific oxidation rate of carbon increased with the NO_2 inlet mole fraction at 350 °C. This increase is linear and the reaction order seems to be close to 1. Thus, the specific rate of carbon consumption by NO_2 in the presence of Ru/Na-Y catalyst may be defined in a similar way as done in the absence of catalyst:

$$r_{dirNO_2} = k_{CO_2}^{cat}X_{NO_2} + k_{CO}X_{NO_2} \qquad (15)$$

Taking in account the depletion of NO_2, one may determine the actual direct oxidation rate of carbon. The experiments of the carbon oxidation by NO_2 in the presence of Ru/Na-Y allow describing the temperature dependence of the kinetic constants
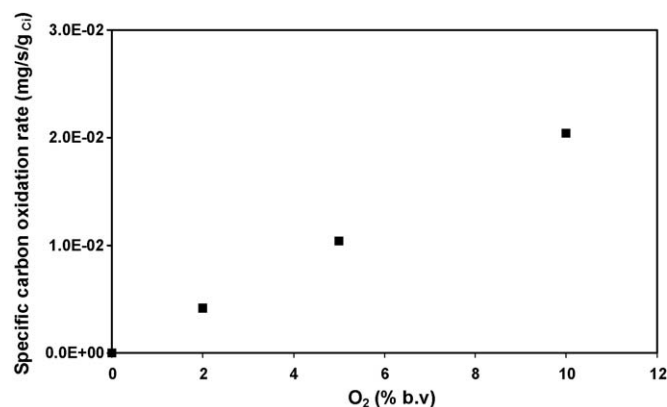

Fig. 2. Influence of the inlet O_2 mole fraction on the specific rate of C–O_2 reaction at 400 °C (■).
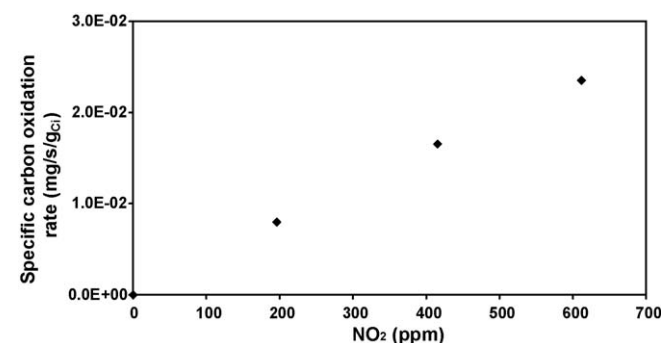

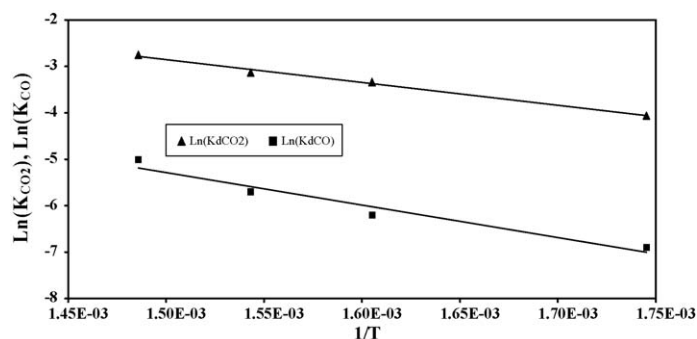**Fig. 3.** Influence of the inlet NO_2 mole fraction on the specific rate of C–NO_2 reaction at 350 °C (■).

Fig. 4. Arrhenius plot of the C–NO$_2$ reaction rate coefficient in the temperature range of 300–400 °C.

$k_{CO_2}^{cat}$ and k_{CO} by an Arrhenius function. The dependence of $k_{CO_2}^{cat}$ and k_{CO} on $1/T$ is shown in Fig. 4. The best fit was obtained for:

$$k_{CO_2}^{cat} = 92.2 \exp\left(-\frac{40900}{RT}\right) (s^{-1}) \tag{16}$$

$$k_{CO} = 182.3 \exp\left(-\frac{58300}{RT}\right) (s^{-1}) \tag{17}$$

A small decrease of the value of the activation energy obtained for the oxidation of carbon by NO$_2$ for $k_{CO_2}^{cat}$ kinetic constant in the presence of Ru/Na-Y catalyst was observed. Such behavior confirmed the catalytic effect of Ru/Na-Y on reaction (6). The activation energy obtained for the oxidation of carbon by NO$_2$ for k_{CO} kinetic constant seemed not to be affected.

4.3. Kinetics of the cooperative C–NO$_2$–O$_2$ in the presence of Ru/Na-Y catalyst

In order to determine the intrinsic rate constants for the catalyzed cooperative reaction, the effect of the NO$_2$ and O$_2$ inlet molar fraction was determined. Specific oxidation rates measured at 350 °C increase with increasing NO$_2$ contents and 10% O$_2$ in the feed gas as shown in Fig. 5. This increase was almost linear which suggests that the partial reaction order in NO$_2$ was close to 1. A different behaviour was previously obtained for Pt based catalyst, on which the reaction order with respect to NO$_2$ for the cooperative reaction was equal to 0.4 [24,25]. That low value was attributed to a reduced dependence of the oxidation rate of carbon on NO$_2$ concentration since NO is continuously oxidized into NO$_2$ in the soot-catalyst layer. This result reveals a different global mechanism of the oxidation of soot by NO$_2$ and O$_2$ in the presence Pt and Ru based catalysts.

The specific carbon oxidation rate in contact with Ru/Na-Y increased with increasing content of O$_2$ keeping constant the NO$_2$
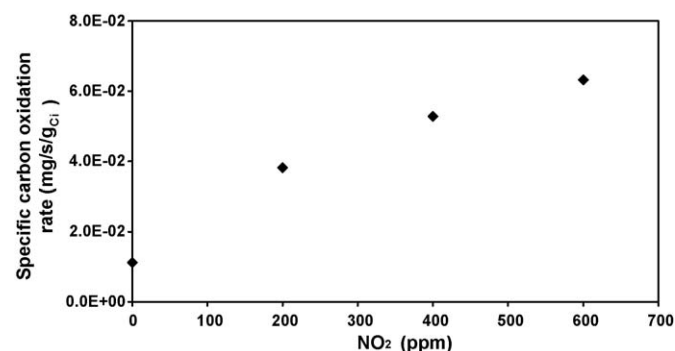

Fig. 5. Influence of the inlet NO$_2$ mole fraction on the specific rate of C–NO$_2$–O$_2$ reaction at 350 °C (■).
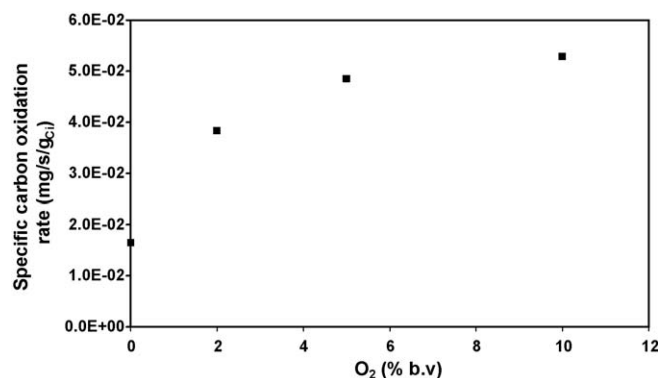

Fig. 6. Influence of the inlet O$_2$ mole fraction on the specific rate of C–NO$_2$–O$_2$ reaction at 350 °C (■).

concentration (Fig. 6). Above 5% O$_2$ in the feed gas the rate of carbon consumption remained almost constant. A similar behavior has already been observed in experiments performed in the absence and in the presence of Pt based catalyst [13,24,25].

Considering the occurring of the direct C–O$_2$, C–NO$_2$ and cooperative C–NO$_2$–O$_2$ reaction when NO$_2$ and O$_2$ were injected simultaneously in the feed gas, one may determine the rate constant of the cooperative reaction which may be written as:

$$r_{coop} = k_{O_2,CO_2}^{cat} X_{NO_2} X_{O_2}^{0.2} + k_{O_2,CO} X_{NO_2} X_{O_2}^{0.2} \tag{18}$$

The best fit for the temperature dependence of the kinetic constants k_{O_2,CO_2}^{cat} and $k_{O_2,CO}$ by an Arrhenius relation was obtained for:

$$k_{O_2,CO_2}^{cat} = 1.28 \times 10^6 \exp\left(-\frac{85250}{RT}\right) (s^{-1}) \tag{19}$$

$$k_{O_2,CO} = 4.05 \times 10^4 \exp\left(-\frac{76210}{RT}\right) (s^{-1}). \tag{20}$$

It is interesting to note that the apparent activation energy for the cooperative reaction leading to CO$_2$ formation (Eq. (8)) was close to the one for the direct C–O$_2$ reaction (Eq. (4)). This result suggested that the direct C–O$_2$ and the cooperative C–NO$_2$–O$_2$ reaction in the presence of Ru/Na-Y catalyst proceeded according to the adsorption of oxygen on carbon surface followed by a decomposition of these oxygenate surface complexes. The formation of this kind of surface complexes was enhanced in the presence of Ru/Na-Y catalyst.

It was observed that the frequency factor was significantly increased for the cooperative reaction compared to the direct C–O$_2$ reaction. This result hints at the important role of NO$_2$ in the decomposition of carbon oxygenate species. The obtained value of
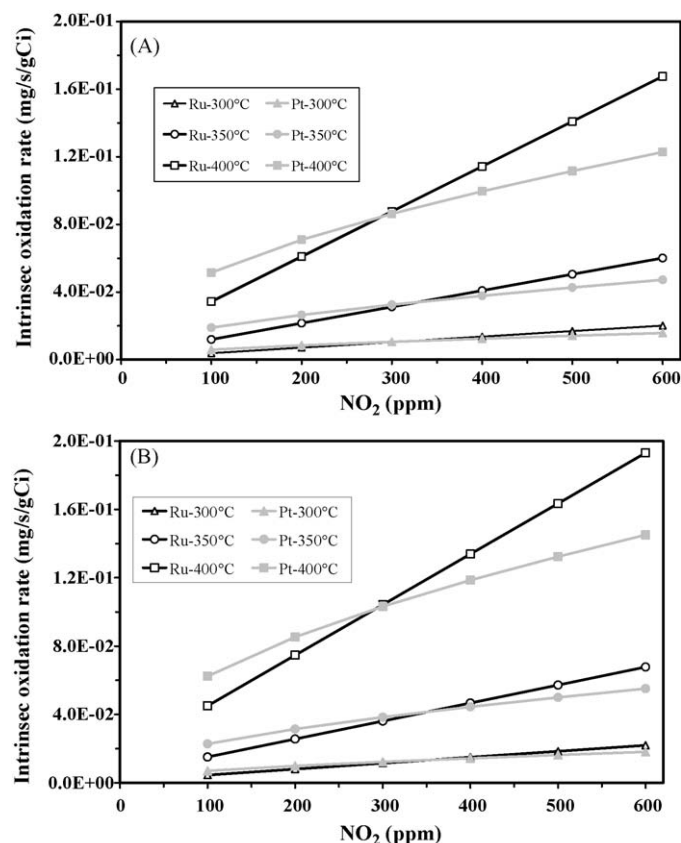
Fig. 7. Comparison between intrinsic oxidation rates of soot oxidation in the presence of Pt and Ru catalysts for different exhaust conditions ((a) 300–400 °C; 100–600 ppm NO$_2$, 5%O$_2$; (b) 300–400 °C; 100–600 ppm NO$_2$, 10%O$_2$).

the activation energy was different from the one previously obtained for a Pt based catalyst (72.1 kJ/mol) [24] and in the absence of catalyst (65.4 kJ/mol). This result confirmed that the global oxidation mechanism of the cooperative reaction in the presence of Ru/Na-Y catalyst is different from the one in the presence of a Pt based catalyst and in the absence of catalyst. In fact, during the cooperative reaction in the absence and in the presence of Pt catalyst, 1 oxygen atom contained in NO$_2$ is consumed for the formation of 1 CO$_2$ molecule. On Ru/Na-Y however, NO$_2$ contributes to the decomposition of oxygenate complexes without providing an oxygen atom. The proposed kinetic models reveal the different behaviors of Pt and Ru based catalyst in carbon oxidation in the presence of NO$_2$ and O$_2$.

Using the obtained kinetic constants, the intrinsic carbon oxidation rate in the presence of Pt and Ru catalyst were compared at different conditions relevant to exhaust gas after treatment (Fig. 7). A Pt catalyst has a higher activity compared to Ru catalyst at NO$_2$ inlet mole fractions below 300 ppmv independent of oxygen inlet concentration. However, the Ru catalyst exhibits a higher activity at NO$_2$ inlet mole fractions above 300 ppmv. These results are in agreement with the proposed catalytic global mechanism of carbon oxidation. At low inlet NO$_2$ concentration, the continuous oxidation of NO into NO$_2$ may explain the higher activity of Pt catalyst. In contrast, in the presence of Ru catalyst little oxidation of NO into NO$_2$ occurred. The concentration of NO$_2$ was insufficient for achieving the decomposition of SOCs. Note that the catalytic global mechanism shows that 1 mole of NO$_2$ is necessary for the decomposition of 1 SOC.

At NO$_2$ inlet concentrations above 300 ppmv, the Ru based catalyst exhibits the highest activity for soot oxidation. Moreover, the activity difference between the Ru and Pt catalyst is increasing

with temperature. There are two explanations for the temperature effect. First, there is a larger contribution of the direct oxidation of carbon by O$_2$ over Ru compared to Pt catalyst. The contribution of C–O$_2$ reactions increases with temperature. Second, the oxidation of NO into NO$_2$ becomes limited owing to the internal thermodynamic equilibrium between NO and NO$_2$ in the presence of O$_2$ being unfavourable for NO$_2$ at higher temperatures. The Pt catalyst is relying on efficient NO into NO$_2$ oxidation [24–29].

The obtained kinetic constants confirm the different global mechanisms obtained during the catalytic oxidation of soot by NO$_2$ and O$_2$ in the presence of Pt and Ru catalysts. The use of the synergetic effects of Ru and Pt in exhaust gas after treatment may be a promising issue for Diesel particle treatment technology.

5. Conclusions

The effect of Ru/Na-Y catalyst on the oxidation of soot by O$_2$ and NO$_2$ was investigated in the temperature range 300–400 °C. Ru based catalyst exhibits a high catalytic activity on the carbon oxidation. The established kinetic equations indicate that the frequency factor is increased for the cooperative reaction comparing the direct C–O$_2$ reaction. This result confirms that the ruthenium surface is a generator of active oxygen species that are transferred to the carbon surface leading to a larger concentration of surface oxygenated carbon complexes. NO$_2$ plays an important role on the decomposition of these complexes leading to an increase in the carbon consumption. The obtained kinetic constants or Pt and Ru are in agreement with different global mechanisms obtained for both catalysts. Hence, an oxidation global mechanism and a kinetic model based on the occurring of direct and cooperative reactions may be applied for the catalytic oxidation of soot in the regenerative particle trap conditions.

References

[1] G.C. Koltsakis, A.M. Stamatelos, Prog. Energy Combust. Sci. 23 (1997) 1.
[2] C. Görsmann, Monat. Chem. 136 (2005) 91.
[3] I.I. Kandylas, O. haralampous, G. Koltsakis, Ind. Eng. Chem. Res. 41 (2002) 5372.
[4] A.P. Walker, Top. Catal. 28 (2004) 165.
[5] H. Lüders, P. Stommel, S. Geckler, Diesel Exhaust Treatment – New Approaches to Ultra Low Emission Diesel Vehicles, SAE paper 1999-01-0108.
[6] P. Richards, M. Papachristos, Diesel Particulate Filters and Fuel-Borne Catalysts as a Viable Solution to Reduced Airborne Particulate, SAE paper 2001-28-0041.
[7] B.J. Cooper, J.E. Thoss, The Role of NO in Diesel Particulate Emission Control, SAE paper 890404, 1989.
[8] B.J. Cooper, H.J. Radnor, W. Jung, J.E. Thoss, Treatment of diesel exhaust gases. US Patent 4,902,487 (1990).
[9] A. Messerer, R. Niessner, U. Pöshl, Carbon 44 (2006) 307.
[10] B. Stanmore, J.F. Brilhac, P. Gilot, Carbon 39 (2001) 2247.
[11] P. Ehrburger, J.F. Brilhac, Y. Drouillot, V. Logie, P. Gilot, Reactivity of Soot with Nitrogen Oxides in Exhaust Stream, SAE Technical paper 2003, 01,1683.
[12] M. Jeguirim, V. Tschamber, J.F. Brilhac, P. Ehrburger, J. Anal. Appl. Pyrol. 72 (2004) 171.
[13] F. Jacquot, V. Logie, J.F. Brilhac, P. Gilot, Carbon 40 (2003) 335.
[14] M. Jeguirim, V. Tschamber, J.F. Brilhac, P. Ehrburger, Fuel 84 (14–15) (2005) 1949.
[15] M. Jeguirim, V. Tschamber, J.F. Brilhac, Int. J. Chem. Kinet. 41 (2009) 236.
[16] J.P. Neeft, M. Makee, J.A. Moulijn, Appl. Catal. B 8 (1996) 57.
[17] P. Ciambelli, V. Palma, P. Russo, S. Vaccaro, Catal. Today 60 (2000) 43.
[18] K. Villani, R. Brosius, J.A. Martens, J. Catal. 236 (2005) 172.
[19] S.J. Jelles, R.R. Krul, M. Makkee, J.A. Moulijn, Catal. Today 53 (1999) 623.
[20] J.O. Uchisawa, A. Obuchi, A. Ogata, R. Enomoto, S. Kushiyama, Appl. Catal. B 21 (1999) 9.
[21] A. Setiabudi, M. Makkee, J.A. Moulijn, Appl. Catal. B 50 (2004) 185.
[22] M. Seipenbusch, J.V. Erven, T. Schalow, A.P. Schalow, A.P. Weber, A.D. Langeveld, J.C.M. Marijnissen, S.K. Friedlander, Appl. Catal. B 55 (2004) 31.

[23] K. Villani, W. Vermandel, K. Smets, L. Duoduo, G. Van Tendeloo, J.A. Martens, Environ. Sci. Technol. 40 (2006) 2727.

[24] M. Jeguirim, V. Tschamber, P. Ehrburger, Appl. Catal. B 76 (2007) 235.

[25] M. Jeguirim, V. Tschamber, J.F. Brilhac, J. Chem. Technol. Biotechnol. 84 (2009) 770.

[26] K. Villani, C. Kirschhock, L. Duoduo, G. Van Tendeloo, J.A. Martens, Angew. Chem. 118 (2006) 3178.

[27] V. Tschamber, M. Jeguirim, K. Villani, J. Martens, P. Ehrburger, Appl. Catal. B 74 (2007) 299.

[28] S. Aouad, E. Saab, E. Abi Aad, A. Aboukaïs, Catal. Today 119 (2007) 273.

[29] M. Jeguirim, V. Tschamber, K. Villani, J.F. Brilhac, J. Martens, Chem. Eng. Technol. 32 (2009) 830.

[30] P.G. Gray, D.D. Do, Chem. Eng. Commun. 125 (1993) 109.